



Publication Year	2000
Acceptance in OA@INAF	2023-02-06T13:30:58Z
Title	Observations and Atmospheric Parameters of Super-Metal-rich Candidates
Authors	Malagnini, M. L.; MOROSSI, Carlo; BUZZONI, Alberto; Chavez, M.
DOI	10.1086/317714
Handle	http://hdl.handle.net/20.500.12386/33176
Journal	PUBLICATIONS OF THE ASTRONOMICAL SOCIETY OF THE PACIFIC
Number	112

Observations and Atmospheric Parameters of Super-Metal-rich Candidates¹

M. L. MALAGNINI

Dipartimento di Astronomia, Università degli Studi di Trieste, via G. B. Tiepolo 11, 34131 Trieste, Italy; and Telescopio Nazionale Galileo, Observatorio Roque de los Muchachos, A.P. 565, 38700 Santa Cruz de La Palma, Canary Islands, Spain

C. MOROSSI

Osservatorio Astronomico di Trieste, via G. B. Tiepolo 11, 34131 Trieste, Italy

A. BUZZONI

Osservatorio Astronomico di Brera, via Bianchi 46, 23807 Merate (Lc), Italy

AND

M. CHAVEZ

Instituto Nacional de Astrofísica, Óptica y Electrónica, A.P. 51 y 216, 72000 Puebla, Mexico

Received 2000 July 4; accepted 2000 August 10

ABSTRACT. The spectroscopic properties of a sample of 92 Population I bright stars ($V < 8$) with literature values of $[\text{Fe}/\text{H}] \geq +0.1$ are reviewed in order to study the metallicity scale at supersolar regimes. For 73 of these candidate super-metal-rich (SMR) stars we identified the photospheric *fiducial* parameters (T_{eff} , $\log g$, $[\text{M}/\text{H}]$) from among published parameter sets via a comparison of new observations in the wavelength range 5034–5398 Å with synthetic spectra derived from the 1997 database of Chavez et al. As a main issue in our analysis, we find that a “genuine” SMR stellar component in the Galactic disk exists with more than one-fourth of the stars in our sample fulfilling the criterion $[\text{Fe}/\text{H}] \geq 0.2$ dex, and three of them as rich as $[\text{Fe}/\text{H}] > +0.4$ dex.

1. INTRODUCTION

Recent systematic observations of stellar populations in external galaxies and local aggregates have been providing extensive evidence for enhanced chemical evolution. The Galactic bulge is probably the most direct example in this sense, with an important fraction of its integrated luminosity supplied by red giant stars whose spectra are line-enhanced compared to the Sun (Whitford & Rich 1983). Preliminary studies of the bulge stellar population agreed in attributing to such stars a mean metallicity larger than solar ($[\text{Fe}/\text{H}] \gtrsim +0.2$), with some objects in excess of $[\text{Fe}/\text{H}] \gtrsim +1$ (Rich 1988; Terndrup, Frogel, & Whitford 1991; Geisler & Friel 1992).

As summarized in McWilliam (1997) and extensively discussed by Taylor (1991, 1994a, 1994b, 1995, 1996, 1999a, 1999b) in a comprehensive series of review papers, the terms and the limits of the definition of super-metal-rich (SMR) stars still need to be further investigated. A central issue hinges around whether very strong lined (VSL) stars are really to be explained in terms of metal excess or rather

demand supplementary physical alternatives. More elaborate interpretation is now reducing the metallicity estimate for the Galactic bulge to less extreme boundary limits, probably not so far from the solar value (McWilliam & Rich 1994; Sadler, Rich, & Terndrup 1996; see Frogel 1999 for a recent review).

Following the original definition of Spinrad & Taylor (1969), also adopted in Taylor’s (1996) general discussion, SMR stars are those exceeding the Hyades metallicity (originally set at $[\text{Fe}/\text{H}] = +0.2$). While setting up any quantitative threshold is just a matter of subjective definition, nonetheless it is clear that we must eventually rely on a comparison with the solar abundance taken as a reference point. In fact, the supermetallicity phenomenon requires detailed comparison of element abundances among the entire pattern of “metallic” elements which is better feasible by assuming the Sun as comparison candle instead of relying on the less exhaustive Hyades data.

There are at least two main difficulties that we should consider in this regard. First of all, it is clear that “metals” are in fact a quite composite family of elements, each of them with its own genesis dealing with supernova processes and/or with the quiescent burning phases inside stellar interiors. Indeed, we know for instance that Population II stars

¹ Based on observations collected at the INAOE “G. Haro” Observatory, Cananea (Mexico).

display a trend of enhanced [O/Fe] at low-Z regimes (Gratton & Ortolani 1986, Barbuy 1988; Abia & Rebolo 1989; Bessell, Sutherland, & Ruan 1991; Edvardsson et al. 1993). This can be regarded as an instructive example of a selective “supersolar” abundance even in a “subsol” chemical framework.

A second difficulty results from the lack of template metal-rich spectra (with the possible controversial exception of μ Leo; see, for example, Castro et al. 1996, and Taylor 1996, 1999c) against which other stars can be calibrated, and so determinations of metal richness rely largely on model atmosphere predictions. The drawback in this case resides in the limits of theory to handle the complex thermodynamic environment in the stellar atmosphere (non-LTE equilibrium, microturbulence, convection, oscillator strengths for a complete set of chemical elements, molecule treatment, etc.).

Big steps have, however, been accomplished by theory in recent years, allowing a fully sophisticated modeling of the spectral energy distribution of stars, especially when restricted to temperatures of $T > 4000$ K (Bell & Gustafsson 1978; Tsuji 1978; Bessell et al. 1989; Buser & Kurucz 1992; Tripicco & Bell 1990, 1995; Kurucz 1979, 1993, hereafter K93). In particular, Kurucz models are recognized as among the few main trusted reference sources for systematic theoretical investigation of stellar atmospheres.

In line with previous work of our group on theoretical synthesis of spectral features in stars (Gulati, Malagnini, & Morossi 1993; Malagnini et al. 1994; Chavez 1995; Chavez, Malagnini, & Morossi 1995, 1996b; Chavez et al. 1996a, 1996c), in this paper we perform a quantitative study of SMR candidates in the solar neighborhood. Our results could thus provide a general interpretative tool to tackle the problem of SMR stellar populations in the Milky Way as well as in external galaxies, via population synthesis studies.

The present work is based on new spectroscopic observations of a large sample of reportedly iron-rich stars in the Galactic disk, according to the current literature. As a primary step in our analysis, we especially intend to focus here on determining preferred values of the atmospheric parameters (effective temperature, surface gravity, overall metallicity) for each star in the sample. This is done by comparing the observed spectra with the appropriate synthetic ones extracted from the grid by Chavez et al. (1997, hereafter CMM). The idea of using moderate-resolution spectra to be compared with synthetic ones instead of carrying out further high-resolution studies of SMR candidates is based on the following considerations: (1) Most high-resolution studies are carried out on very narrow wavelength ranges, thus making impossible the actual determination of T_{eff} . The use of “external” T_{eff} values is in fact one of the main causes of the spread in the metallicity results reported in the literature. With our approach we are able to check simultaneously T_{eff} , $\log g$, and [Fe/H].

(2) Errors in the atomic data may play a very critical role in high-resolution analyses, in particular when only few lines are analyzed, while they may be washed out by using a much larger number of features as in the case of comparing the observed spectra as a whole. (3) The amount of time and effort needed to cover at high resolution a significant number of objects for creating a stellar library for population synthesis work is so high that it practically prevents this kind of approach. And (4) the moderate-resolution approach is directly applicable to studies of the case of external galaxies.

Our model output will eventually serve as a reference framework in a following paper (A. Buzzoni, M. Chavez, M. L. Malagnini, & C. Morossi 2000, in preparation) to match the Lick narrowband spectrophotometric indices (Burstein et al. 1984; Worthey et al. 1994), and calibrate them versus metallicity.

We arrange our work by presenting first the observational database in § 2 and the comparison between synthetic spectra and observations in § 3. Section 4 is devoted to the discussion of our results in terms of [Fe/H] for the stellar sample as a whole and for individual objects. Our conclusions are given in § 5.

2. OBSERVATIONS AND DATA REDUCTION

Our list of candidate SMR stars is derived from the general catalog of Cayrel de Strobel et al. (1997, hereafter CAY97), which represents the most complete and updated collection of [Fe/H] determinations from high-resolution analyses. The target stars were selected by applying a conservative selection criterion, i.e., stars with $[\text{Fe}/\text{H}] \geq +0.1$ dex in *at least* one of the determinations reported in CAY97.² Our sample eventually comprised 92 bright stars in the spectral range between F and M, luminosity class between I and V, and apparent magnitude $V < 8$ mag. The 91 stars of the final sample³ are listed by HD number in Table 1.

For the 91 stars, CAY97 lists 210 individual complete data sets of atmospheric parameters (T_{eff} , $\log g$, [Fe/H]) and 11 other data sets with no indication of $\log g$. Among the 88 stars with assigned luminosity class, there are 55 objects of spectral types F and G, and 33 of types K and M. The first group has a majority of dwarfs (67%), while the second one is composed almost exclusively of evolved stars (88%). This working sample was observed during three runs at the 2.12 m f/12 telescope of the INAOE “G. Haro”

² Only determinations derived by using the Sun as a standard star are considered.

³ Out of the 92 stars, one (HD 197963) was discarded because of contamination of its observed spectrum by a close companion.

TABLE 1
OBSERVATIONAL DATABASE AND ATMOSPHERIC PARAMETERS

HD (1)	Spectral Class (2)	Object Type ^a (3)	V (4)	B-V (5)	T _{eff} (K) (6)	log g (7)	[Fe/H] (8)	n (9)	σ _{obs} (10)	rmse (11)	C ² (12)
4	F0	**	7.78	0.43	6380	3.01	0.3	1	0.03	0.027	0.79
1461 ^b	G0 V	PM	6.46	0.68	5929	4.	0.43	2	0.011	0.021	3.56
1461 ^b					5929	4.5	0.43	2	0.011	0.07	
1835	G3 V	V	6.38	0.67	5860	4.4	-0.09	2	0.025	0.025	
1835					5793	4.5	0.19	2	0.025	0.018	0.51
1835					5860	4.4	0.28	2	0.025	0.019	
1835					5793	4.6	0.24	2	0.025	0.02	
1835					5793	4.5	0.2	2	0.025	0.018	
1835					5673	4.22	-0.01	2	0.025	0.019	
4188	K0 III	V	4.76	1.01	4755	2.9	0.15	3	0.015	0.078	
4188					4790	2.9	-0.16	3	0.015	0.054	12.05
8673	F7 V	PM	6.31	0.47	6380	4.5	0.16	3	0.008	0.017	4.1
10307	G1.5 V	PM	4.90	0.67	5793	4.38	-0.03	3	0.016	0.018	
10307					5898	4.31	-0.02	3	0.016	0.017	1.08
10307 ^b					5929	4.	+0.20	3	0.016	0.019	
10307 ^b					5929	4.5	+0.20	3	0.016	0.020	
10307 ^b					6000	4.	+0.14	3	0.016	0.019	
10307 ^b					6000	4.5	+0.14	3	0.016	0.017	
10307 ^b					6000	4.	+0.16	3	0.016	0.019	
10307 ^b					6000	4.5	+0.16	3	0.016	0.017	
10780	K0 V	PM	5.63	0.81	5419	4.6	0.36	3	0.01	0.03	8.26
16232	F6 V		6.50	0.41	6462	4.5	0.27	2	0.011	0.019	2.59
18322	K1 III	V	3.89	1.11	4710	2.8	0.2	2	0.013	0.048	
18322					4710	2.8	0.21	2	0.013	0.049	
18322					4600	2.84	-0.23	2	0.013	0.038	8.98
19476	K0 III	V	3.80	0.98	4941	3.3	0.08	4	0.015	0.031	
19476					4941	3.3	0.08	4	0.015	0.031	
19476					4990	2.68	0.19	4	0.015	0.033	
19476					4940	3.08	0.04	4	0.015	0.027	3.05
20630	G5 Vvar	V	4.83	0.68	5663	4.45	0.08	2	0.018	0.021	
20630					5663	4.4	-0.01	2	0.018	0.02	1.14
20630					5600	4.5	0.04	2	0.018	0.023	
20630					5667	4.29	-0.01	2	0.018	0.02	
20675 ^b	F6 V	PM	5.93	0.43	6545	4.	0.2	3	0.01	0.013	1.4
20675 ^b					6545	4.5	0.2	3	0.01	0.014	
26846	K3 III	**	4.86	1.18	4500	2.54	0.09	3	0.009	0.045	
26846					4582	2.7	0.21	3	0.009	0.042	20.23
26846					2710	4.1	0.19	3	0.009	0.488	
27371	K0 III	V	3.65	0.99	4800	2.6	0.09	3	0.013	0.041	
27371					4930	2.9	-0.02	3	0.013	0.033	6.47
27371					4900	2.6	0.13	3	0.013	0.039	
30495	G3 V	PM	5.50	0.64	6000	4.5	0.1	2	0.006	0.029	23.48
30495					5829	4.3	-0.13	2	0.006	0.029	
30562	F8 V	PM	5.77	0.63	5860	3.75	0.13	2	0.007	0.021	
30562					5886	3.98	0.14	2	0.007	0.02	7.65
30652	F6 V	V	3.19	0.45	6462	4.5	-0.69	3	0.009	0.029	
30652					6380	4.4	0.02	3	0.009	0.011	1.62
32068	K4 Ib-II+...	AI	3.75	1.25	4032	1.35	0.3	2	0.02	0.098	
32068					4200	1.15	0.1	2	0.02	0.057	8.91
32068					3920	1.33	-0.26	2	0.02	0.109	
33276	F2 IV	**	4.82	0.32	7099	3.3	0.29	2	0.015	0.02	1.77
34411	G1.5 IV-V	PM	4.70	0.64	5860	4.11	0.35	2	0.007	0.02	
34411					5860	4.1	0.3	2	0.007	0.018	
34411					5860	4.3	0.06	2	0.007	0.013	3.2

TABLE 1—Continued

HD (1)	Spectral Class ^a (2)	Object Type (3)	V (4)	B-V (5)	T _{eff} (K) (6)	log g (7)	[Fe/H] (8)	n (9)	σ _{obs} (10)	rmse (11)	C ² (12)
34411.....					5860	4.16	-0.08	2	0.007	0.015	
34411.....					5845	4.22	0.1	2	0.007	0.014	
34411.....					5889	4.12	-0.03	2	0.007	0.015	
35620.....	K3 III CN+...	**	5.08	1.40	4200	1.	-0.42	1	0.03	0.054	
35620.....					4200	1.5	-0.09	1	0.03	0.041	1.89
35620.....					4200	2.15	0.11	1	0.03	0.074	
35620.....					4200	1.5	0.05	1	0.03	0.046	
36389.....	M2 Iab:	sr	4.49	1.92	3706	0.7	0.11	2	0.152	0.252	3.02
37387.....	K1 Ib	**	7.48	1.94	4500	1.2	0.13	1	0.03	0.091	10.76
37763.....	K2 III	PM	5.17	1.15	5040	3.3	0.4	1	0.03	0.057	
37763.....					4624	2.4	0.3	1	0.03	0.04	1.77
44391.....	K0 Ib		7.74	1.40	4710	0.6	0.21	2	0.023	0.061	7.5
45412.....	F8 Ibvar	Ce	5.55	0.68	6632	1.5	0.1	2	0.01	0.045	19.19
48682 ^b	G0 V	**	5.27	0.55	5727	4.	0.15	2	0.018	0.032	3.33
48682 ^b					5727	4.5	0.15	2	0.018	0.04	
52973.....	G0 Ibvar	Ce	3.79	0.79	5727	1.5	0.49	2	0.017	0.033	3.62
52973.....					5727	1.5	0.21	2	0.017	0.035	
52973.....					5727	1.9	0.33	2	0.017	0.033	
56577.....	K4 III	**	4.78	1.70	4500	1.35	0.15	1	0.03	0.125	20.
58207.....	G9 IIIb		3.79	1.03	4770	2.92	-0.17	2	0.014	0.027	3.96
58207.....					4725	2.15	-0.07	2	0.014	0.03	
58207 ^b					4421	3.	+0.16	2	0.014	0.134	
58207 ^b					4421	3.5	+0.16	2	0.014	0.168	
59881.....	F0 III		5.20	0.27	7636	3.07	0.19	3	0.017	0.017	0.91
61064.....	F6 III	dS	5.10	0.47	6380	3.21	0.44	2	0.024	0.018	0.58
63302.....	K3 Iab/Ib	V	6.34	1.78	4500	0.2	0.17	1	0.03	0.109	14.67
63700.....	G6 Ia	**	3.35	1.25	4990	1.15	0.24	1	0.03	0.07	5.5
74739.....	G8 Iab:	**	4.02	1.01	4846	2.	0.2	2	0.026	0.039	
74739.....					4900	2.2	-0.07	2	0.026	0.028	
74739.....					4960	2.69	-0.14	2	0.026	0.026	0.97
75732.....	G8 V	PM	5.95	0.87	5196	4.4	0.11	3	0.012	0.026	
75732.....					5196	4.5	0.24	3	0.012	0.026	4.39
75732.....					5196	4.5	0.3	3	0.012	0.027	
81029.....	F0	**	7.31	0.31	7304	3.95	0.27	1	0.03	0.026	0.74
82734.....	K0 III		5.01	1.02	4990	3.11	0.4	1	0.03	0.043	2.16
83951.....	F3 V		6.14	0.36	6720	4.	0.14	2	0.01	0.014	1.97
83951.....					6789	4.11	-0.02	2	0.01	0.014	
83951.....					6840	4.	0.03	2	0.01	0.014	
85503.....	K2 III	PM	3.88	1.22	4460	2.4	-0.01	2	0.017	0.034	4.12
85503.....					4421	2.3	-0.11	2	0.017	0.035	
85503.....					4421	2.3	0.03	2	0.017	0.036	
85503.....					4541	2.35	0.48	2	0.017	0.041	
85503.....					4710	2.82	0.11	2	0.017	0.046	
85503.....					4541	2.3	0.35	2	0.017	0.036	
85503.....					4480	2.61	0.17	2	0.017	0.04	
85503.....					4308	2.2	0.31	2	0.017	0.079	
85503.....					4540	2.3	0.42	2	0.017	0.038	
85503.....					4375	1.95	0.12	2	0.017	0.039	
87822.....	F4 V	**	6.24	0.45	6545	4.2	0.19	2	0.019	0.015	0.62
87822.....					6650	4.	0.16	2	0.019	0.017	
88230.....	K8 V	V	6.61	1.37	4000	4.5	0.28	2	0.03	0.168	31.08
88284.....	K0 III	SB	3.61	1.01	5091	3.12	0.09	1	0.03	0.041	1.79
88284.....					4890	2.99	0.05	1	0.03	0.049	
88284.....					4850	2.55	0.12	1	0.03	0.053	
90277.....	F0 V		4.70	0.29	7412	3.46	0.19	2	0.018	0.017	0.89
92125.....	G2.5 IIa		4.70	0.82	5220	2.12	-0.24	2	0.028	0.026	0.81

TABLE 1—Continued

HD (1)	Spectral Class (2)	Object Type ^a (3)	V (4)	B-V (5)	T _{eff} (K) (6)	log g (7)	[Fe/H] (8)	n (9)	σ _{obs} (10)	rmse (11)	C ² (12)
92125					5600	2.1	0.38	2	0.028	0.027	
95272	K1 III	PM	4.07	1.10	4800	3.01	0.1	1	0.03	0.032	
95272					4650	2.8	-0.22	1	0.03	0.029	0.96
100563	F5 V	PM	5.70	0.53	6380	4.3	0.12	2	0.019	0.023	1.45
102634	F7 V	PM	6.15	0.52	6072	4.3	0.14	2	0.012	0.019	
102634					6072	4.3	0.1	2	0.012	0.018	2.31
102634					6387	4.18	0.24	2	0.012	0.021	
102870	F9 V	PM	3.61	0.55	6146	4.29	0.26	2	0.009	0.016	
102870					6072	4.12	0.28	2	0.009	0.017	
102870					6000	4.3	0.29	2	0.009	0.021	
102870					6146	4.3	0.2	2	0.009	0.016	
102870					6146	4.3	0.2	2	0.009	0.016	
102870					6146	4.4	0.14	2	0.009	0.016	
102870					6072	4.1	0.18	2	0.009	0.015	2.68
102870					6146	4.2	0.1	2	0.009	0.016	
102870					6190	4.2	0.1	2	0.009	0.017	
102870					6176	4.14	0.13	2	0.009	0.016	
104304	G9 IV	PM	5.54	0.78	5478	4.24	0.18	2	0.01	0.021	4.37
109511	K2 III	V	5.02	1.15	4480	2.5	-0.09	2	0.019	0.054	8.46
109511 ^b					7875	3.	+0.42	2	0.019	0.139	
109511 ^b					7875	3.5	+0.42	2	0.019	0.137	
113022	F6 Vs	PM	6.20	0.42	6380	4.2	0.1	1	0.03	0.022	0.53
114710	F9.5 V	PM	4.26	0.57	5929	4.47	0.27	1	0.03	0.025	
114710					6146	4.52	0.06	1	0.03	0.021	
114710					5929	4.4	0.02	1	0.03	0.019	0.39
114710					6029	4.38	0.03	1	0.03	0.019	
115604	F3 III	V	4.73	0.30	7522	4.1	0.44	1	0.03	0.034	
115604					7875	3.8	0.32	1	0.03	0.04	
115604					7200	3.	0.18	1	0.03	0.032	1.14
120136	F6 IV	V	4.50	0.48	6462	4.3	0.28	1	0.03	0.02	
120136					6380	4.3	0.14	1	0.03	0.019	0.39
120136					6380	3.8	0.3	1	0.03	0.021	
120136					6462	4.3	0.	1	0.03	0.026	
121370	G0 IV	SB	2.68	0.58	6222	3.8	0.16	1	0.03	0.028	
121370					6219	4.01	0.3	1	0.03	0.023	
121370					6000	3.83	0.16	1	0.03	0.021	0.48
121370					6068	3.83	0.19	1	0.03	0.022	
124570	F6 IV	SB	5.50	0.58	6222	4.2	0.	1	0.03	0.026	
124570					6222	4.2	0.12	1	0.03	0.025	0.71
124570					6222	4.2	0.13	1	0.03	0.025	
124570					6237	4.04	0.07	1	0.03	0.026	
129989	K0 II-III	**	2.70	0.97	4730	2.24	-0.13	1	0.03	0.034	1.35
129989					4800	2.2	0.36	1	0.03	0.045	
130948 ^b	G1 V		5.85	0.56	5727	4.	0.2	1	0.03	0.025	0.69
130948 ^b					5727	4.5	0.2	1	0.03	0.033	
140573	K2 IIIb	**	2.65	1.17	4541	2.5	0.23	1	0.03	0.042	2.08
140573					4624	2.39	-0.07	1	0.03	0.056	
140573					4582	2.9	0.37	1	0.03	0.053	
140573					4582	2.	0.17	1	0.03	0.046	
140573					4530	2.76	0.03	1	0.03	0.042	
140573					4475	1.75	-0.05	1	0.03	0.044	
144284	F8 IV	SB	4.01	0.52	6309	4.13	0.2	4	0.014	0.013	0.82
145675	K0 V	PM	6.67	0.90	5196	4.4	0.18	2	0.022	0.025	1.26
145675					5196	4.5	0.22	2	0.022	0.027	
145675					5250	4.57	0.35	2	0.022	0.029	
145675					5419	4.5	0.31	2	0.022	0.032	
146051	M0.5 III	V	2.74	1.58	3679	1.4	0.32	2	0.019	0.212	132.39

TABLE 1—Continued

HD (1)	Spectral Class (2)	Object Type ^a (3)	V (4)	B-V (5)	T _{eff} (K) (6)	log g (7)	[Fe/H] (8)	n (9)	σ _{obs} (10)	rmse (11)	C ² (12)
150680.....	G0 IV	SB	2.81	0.65	5740	3.7	-0.07	2	0.012	0.016	1.62
150680.....					5825	3.78	0.05	2	0.012	0.016	
156283.....	K3 Iab:		3.16	1.44	5419	4.1	0.32	2	0.022	0.101	
156283.....					4100	1.68	-0.18	2	0.022	0.076	12.26
157881.....	K7 V	PM	7.54	1.36	4000	4.5	0.4	2	0.015	0.163	126.08
159181.....	G2 Iab:	**	2.79	0.98	5362	1.35	0.29	2	0.017	0.035	
159181.....					5362	1.6	0.1	2	0.017	0.036	
159181.....					5362	1.35	0.3	2	0.017	0.035	
159181.....					5250	1.6	0.14	2	0.017	0.033	4.04
160922 ^b	F5 V	SB	4.80	0.43	6720	4.	0.4	2	0.02	0.013	0.37
160922 ^b					6720	4.5	0.4	2	0.02	0.013	
161096.....	K2 III		2.77	1.16	4624	2.44	0.14	2	0.034	0.028	0.68
161096.....					4550	2.63	0.02	2	0.034	0.037	
161096.....					4475	1.7	0.	2	0.034	0.035	
161797.....	G5 IV	PM	3.41	0.76	5538	3.91	0.16	3	0.012	0.017	2.07
161797.....					5419	4.1	0.3	3	0.012	0.028	
161797.....					5419	4.1	0.32	3	0.012	0.029	
161797.....					5520	3.7	0.04	3	0.012	0.019	
162917.....	F4 IV–V		5.70	0.49	6380	4.1	0.1	4	0.011	0.013	1.34
163770.....	K1 IIaCN+...		3.82	1.39	4700	1.4	0.25	1	0.03	0.064	
163770.....					4330	1.28	-0.24	1	0.03	0.052	3.23
163993.....	G8 III		3.70	0.94	4990	2.5	0.27	3	0.012	0.04	
163993.....					5030	2.92	-0.1	3	0.012	0.02	2.57
167858 ^b	F2 V		6.63	0.31	7000	4.	0.17	3	0.015	0.013	0.79
167858 ^b					7000	4.5	0.17	3	0.015	0.013	
171802.....	F5 III		5.39	0.37	6462	4.2	0.1	2	0.007	0.016	4.8
181276.....	G9 III		3.80	0.93	5040	2.59	0.11	2	0.012	0.032	
181276.....					5000	2.95	-0.08	2	0.012	0.024	4.1
182572.....	G8 IV...	V	5.16	0.77	5663	4.26	0.5	2	0.009	0.024	
182572.....					5727	4.13	0.44	2	0.009	0.022	
182572.....					5727	4.6	0.39	2	0.009	0.025	
182572.....					5663	4.	0.21	2	0.009	0.024	
182572.....					5380	3.92	0.15	2	0.009	0.021	5.9
186408.....	G1.5 Vb	PM	5.96	0.64	5929	4.3	0.	2	0.009	0.02	
186408.....					5778	4.29	0.06	2	0.009	0.019	3.9
187238.....	K3 Ia0–Ia...		7.10	2.04	4500	0.8	0.2	3	0.013	0.103	76.73
187299.....	G5 Ia0–Ia...	SB	7.12	1.60	4990	2.1	0.16	2	0.012	0.066	32.43
187691.....	F8 V	PM	5.10	0.56	6146	4.4	0.1	2	0.008	0.014	
187691.....					6146	4.4	0.13	2	0.008	0.014	
187691.....					6146	4.4	0.14	2	0.008	0.014	
187691.....					6146	4.14	0.09	2	0.008	0.013	2.62
187921.....	G2.5: Iab	Ce	6.73	1.15	6000	1.	0.28	3	0.023	0.116	29.35
196725.....	K3 Iab:		5.72	1.53	4500	1.3	0.22	2	0.016	0.057	13.62
197039.....	F5		6.74	0.44	6545	4.5	0.15	2	0.008	0.013	2.88
197572.....	F7 Ib...	Ce	6.87	-0.22	5478	0.4	0.15	4	0.013	0.048	15.32
198084.....	F8 IV–V	PM	4.51	0.54	6146	3.6	0.19	2	0.007	0.015	
198084.....					6188	4.13	0.12	2	0.007	0.014	3.73
201078.....	F7.5 Ib–IIvar	Ce	5.82	0.56	6222	1.8	0.13	2	0.009	0.019	4.21
205512.....	K1 III		4.90	1.08	4941	2.8	0.2	2	0.011	0.028	6.21
205512.....					4165	2.5	0.12	2	0.011	0.184	
205512.....					4630	2.76	-0.08	2	0.011	0.04	
205512.....					4625	1.95	-0.12	2	0.011	0.03	
209750.....	G2 Ib	**	2.90	1.04	5091	1.45	0.03	2	0.011	0.047	
209750.....					5305	1.4	0.31	2	0.011	0.045	
209750.....					5305	1.4	0.14	2	0.011	0.038	12.72
209750.....					5305	1.4	0.3	2	0.011	0.044	
209750.....					5250	1.15	0.1	2	0.011	0.039	

TABLE 1—Continued

HD (1)	Spectral Class (2)	Object Type ^a (3)	V (4)	B-V (5)	T _{eff} (K) (6)	log g (7)	[Fe/H] (8)	n (9)	σ _{obs} (10)	rmse (11)	C ² (12)
216228.....	K0 III		3.52	1.05	4990	3.35	0.09	2	0.009	0.028	9.23
216228.....					4800	1.92	0.14	2	0.009	0.042	
216228.....					4770	2.97	-0.12	2	0.009	0.031	
216228.....					4675	2.15	0.02	2	0.009	0.039	
221148.....	K3 IIIvar	V	6.25	1.09	4710	2.6	0.07	2	0.012	0.05	
221148.....					4450	2.45	0.09	2	0.012	0.044	13.54
221148.....					4450	2.45	0.11	2	0.012	0.045	

^a Notation ** from CAY97.^b Tentative values based on the luminosity classes were assumed for the data lacking log g estimates for 22 composite data sets.

Observatory in Cananea (Mexico). Observations on six nights were accomplished between 1995 December and 1996 August collecting mid-dispersion (35 \AA mm^{-1}) spectroscopic data for the whole sample of stars. The telescope was equipped with a Boller & Chivens spectrograph working with a $600 \text{ groove mm}^{-1}$ grating in the range $4600\text{--}5500 \text{ \AA}$ at mid-resolution (2.5 \AA FWHM at 5000 \AA blazing or $R = \lambda/\Delta\lambda = 2000$ inverse resolution). The detector was a 1024×1024 back-illuminated Tektronix CCD with $24 \mu\text{m}$ pixel size. This provided a plate scale of $0.83 \text{ \AA pixel}^{-1}$ in the wavelength direction and $0.^{\circ}45 \text{ pixel}^{-1}$ in the spatial direction. Of the total sample, 70 stars had two or more observations on different nights, while 22 stars were observed only once. Multiple observations allowed us a fair estimate of the internal accuracy of the whole data set. Each star frame was also accompanied by a calibration spectrum of a reference He-Ar lamp; standard stars from the list of Gutiérrez-Moreno et al. (1988) were observed several times during each night to allow relative flux calibration. Various bias frames were obtained throughout to check CCD response stability, and halogen lamp continuum flat-field frames were collected each night by illuminating the dome. Seeing conditions were not exceptional, reaching typically $1.^{\circ}6\text{--}1.^{\circ}8$ FWHM throughout the different observing runs. This, however, is not a problem given the brightness of the target stars. A signal-to-noise ratio (S/N) in the range 50–200 was typically achieved in the 185 observed spectra. The relevant information on the observational database is summarized in Table 1. For each star, columns (1)–(5) report HD number, spectral type, object type, apparent visual magnitude, and $B-V$ color from CAY97. Columns (6)–(8) give the atmospheric parameter determinations, again from CAY97. Tentative values based on the luminosity classes were assumed for the data sets lacking log g estimates and 22 “composite” data sets (marked by asterisks in Table 1) were derived. Columns (9) and (10) contain the number of observations and the mean internal noise, $\sigma_{\text{obs}} = \sigma(\text{flux})$, computed from repeated observations as the average of the punctual standard deviation of different

spectra of the same object over the whole sampled spectrum.

Data analysis was performed with the IRAF software package developed at NOAO (Image Reduction and Analysis Facility 1992). The ONEDSPEC routines were used in the data processing.

Original spectra were bias-subtracted and corrected for the high-frequency CCD quantum efficiency pattern by dividing by a normalized flat-field frame. Sky and possible scattered light was then subtracted by fitting a plane across the stellar spectrum, and CCD rows in the central FWHM spatial profile of the star were co-summed to obtain a one-dimensional spectrum. Wavelength calibration was accomplished by comparison with the He-Ar lamp reference spectrum to derive the pixel/wavelength dispersion function, and the mean CCD response curve in the relevant wavelength range was obtained for each night from the observation of the standard stars. Relative flux calibration was eventually accomplished by dividing the λ -calibrated one-dimensional spectra by the appropriate mean CCD response curve; data were then rebinned to a fixed $\Delta\lambda \text{ pixel}^{-1}$ to preserve counts/flux linearity. A good wavelength calibration was achieved with a typical rms uncertainty of $\pm 0.02 \text{ \AA}$ throughout the sampled stellar spectrum.

Correction of stellar data for individual Doppler shift was done by fitting the barycenters of three roughly equispaced strong features, namely, Fe I $\lambda 4668.30$, H β (4861.32 \AA), and Mg b (5183.62 \AA). After normalization to the rest frame, spectra were rebinned to a fixed $0.830 \text{ \AA pixel}^{-1}$ step. The whole tuning procedure led to a final uncertainty in wavelength calibration of $\sigma(\lambda) = 0.09 \text{ \AA}$ or $\pm 5 \text{ km s}^{-1}$ in radial velocity.

For the subsequent analysis, multiple observations of each star were co-summed after calibration to obtain one mean spectrum for each object.

Any significant contamination by spectrograph scattered light along the dispersion direction, which would partially fill the spectral lines, was checked and ruled out by comparing our spectra with those from the Library of Medium-

Resolution Fiber Optic Echelle Spectra of F, G, K, and M Field Dwarfs to Giant Stars (Montes, Ramsey, & Welty 1999), kindly provided to us by D. Montes.

3. SYNTHETIC SPECTRA AND *FIDUCIAL* PARAMETERS FOR THE SAMPLE STARS

Fiducial sets of atmospheric parameters⁴ for each star in our sample were derived via a direct comparison of the observed spectra with the CMM theoretical database. This database consists of a collection of high-resolution ($R = 250,000$) synthetic spectra in the range of temperature between 4000 and 8000 K, surface gravity between 1.0 and 5.0 dex, and metallicity [M/H] between -1.0 and $+0.5$ dex.

The line list used in the computations was derived from the atomic and molecular line lists compiled by Kurucz and colleagues. From the original lists, containing information on about 58 million lines of atoms up to the tenth stage of ionization and of diatomic molecules, about 45,000 lines falling in the observed wavelength interval were extracted from a synthetic spectrum computed with the solar parameters. A list of additional lines, which do not play any role in the solar spectrum, but are important in the spectra of cool stars, was derived from the line list used by Gulati (1991). In particular, CN, C₂, MgH, SiH, and CH account for approximately 85% of the $\sim 60,000$ lines so achieved (see Chavez 1995 for full details).

The synthetic spectra adopt for the Sun the element abundances from Anders & Grevesse (1989) to be consistent with the Kurucz models; in particular, the solar iron abundance is $\epsilon(\text{Fe}) = 7.63$ dex.

An approximate quantitative estimate of the relative importance of the absorption due to Fe in the observed wavelength range with respect to the total absorption was obtained by artificially removing the Fe features in the computation of some representative synthetic spectra. It results that the relative importance of Fe blanketing ranges from 15% of the total for the (4500, 4.0, +0.5) model to 50% for the solar model. The reduced relative importance of atomic Fe in the spectrum of the cooler model reflects the increasing importance of molecular absorption at low T_{eff} . The above-quoted figures are only a convenient approximation, since the same model atmospheres were used in computing synthetic spectra with and without Fe lines, thus introducing a certain level of internal inconsistency in the latter case. As far as the other main absorbers are concerned, we

notice that most of the C atomic and molecular features fall in the blue part ($\lambda < 5165.5 \text{ \AA}$) of the spectral region under analysis.

To match the observations, the original grid of synthetic spectra was modified accordingly by degrading the original resolution to $\text{FWHM} = 2.5 \text{ \AA}$ via Gaussian filtering, and by rebinding each spectrum at the 663 wavelength points between 4850.89 and 5400.35 \AA of the observational data set. The convolution kernel used to degrade the synthetic spectra was derived by fitting several unblended lines in the He-Ar lamp reference spectra. No correction was required to account for rotational line broadening, since late-type stars are known to be slow rotators, and no peculiar cases resulted from direct inspection of the observed data. For each star as many synthetic spectra as the number of parameter sets reported in Table 1 were derived from the CMM grid by interpolating linearly in the three-dimensional space (T_{eff} , $\log g$, [M/H]). It is worth noting that we used the overall metallicity parameter [M/H] as representative of the observed [Fe/H], thus assuming a solar chemical partition for the heavy elements.

Although the comparison could in principle take advantage of the whole spectral window of observations, the adequacy of CMM synthetic spectra may sensibly vary along the wavelength range (Chavez 1995). A preliminary test in this sense was performed by using as a benchmark the high-resolution spectrum of the Sun by Kurucz et al. (1984) degraded and rebinned to match our observations. Figure 1 shows the residuals ΔFlux of the benchmark spectrum with respect to the synthetic one computed with the solar parameters (T_{eff} , $\log g$, [M/H]) = (5777, 4.4377, 0.0). Shortward of 5034 \AA , a systematic drift is evident from the figure, very likely due to a poor modeling of H β (Gulati 1989; Castelli, Gratton, & Kurucz 1997) and to discrepancies in the Lick Fe5015 bandpass (see discussion in Chavez 1995, § 3.2). The

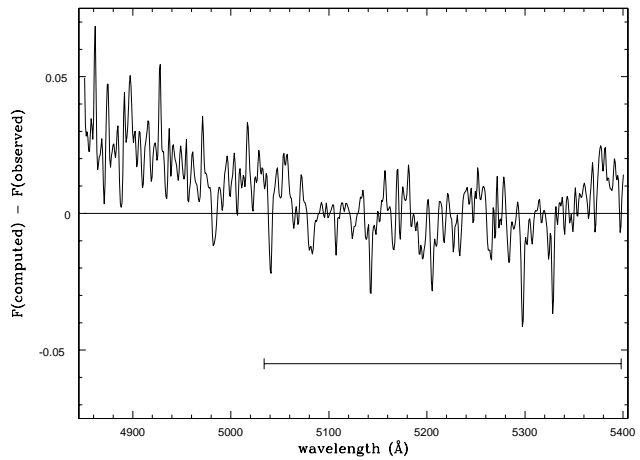


FIG. 1.—Difference between computed and observed absolute flux for the solar spectrum, degraded and rebinned according to the characteristics of the program stars spectra. The 5034–5398 \AA interval is indicated.

⁴ In the following the term *fiducial* is used to identify the parameter sets which are from literature high-resolution studies and are consistent with our observations.

analysis of the residuals shows that no systematic trends are present in the 5034–5398 Å range. On the basis of this analysis, to be conservative, we decided to restrain our comparison for the whole sample of spectra to the above-mentioned range.

In order to obtain for each star the *fiducial* T_{eff} , $\log g$, and [M/H], we computed the rms error (rmse; col. [11] in Table 1) between the observed and each synthetic spectrum after a normalization to their mean values to get rid of scaling problems. The *fiducial* parameters are identified on the basis of the minimum rms error value, rmse_{min} (although for stars with only one CAY97 determination there is actually no real choice).

3.1. Accuracy of the (T_{eff} , $\log g$, [M/H]) Solution

A plot of the rmse_{min} values versus fiducial T_{eff} and $\log g$ is illustrated in Figure 2. The value of rmse_{min} increases with decreasing temperature (*panel a*), and the trend becomes more evident below 4500 K with higher rmse_{min} for both high- and low-gravity stars. This is likely due to intrinsic physical limits in the CMM database at lower temperatures. We recall also that *fiducial* T_{eff} below 4000 K and/or *fiducial* $\log g$ below 1.0 dex compelled us to derive synthetic spectra by extrapolating off rather than interpolating in the CMM grid.

Even if there are strong indications of nonnormality of the residuals used to compute rmse_{min}, we decided to use

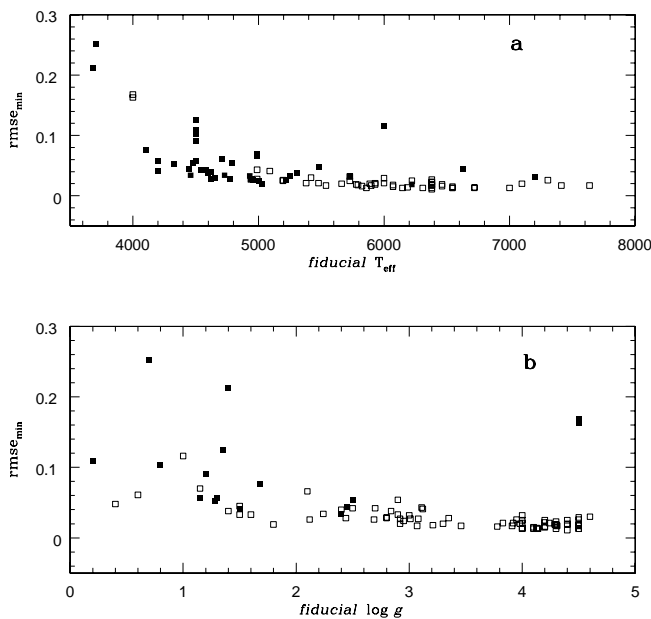


FIG. 2.—Values of rmse_{min} vs. *fiducial* effective temperature (*a*) and *fiducial* surface gravity (*b*). Filled symbols correspond to stars with $\log g \leq 3$ dex in panel *a*, and to stars with $T_{\text{eff}} \leq 4500$ K in panel *b*, respectively.

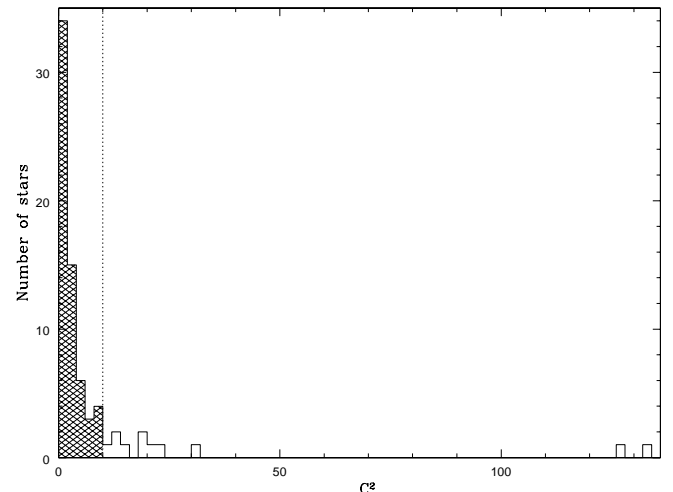


FIG. 3.—Histogram of C^2 values from Table 1; the shaded area corresponds to stars with $C^2 \leq 10$.

the normalized χ^2 quantity in order to give a relative estimate of the goodness of the *fiducial* sets. Therefore, only for the *fiducial* sets identified by rmse_{min}, we computed and listed in Table 1 (col. [12]) the quantity C^2 . We used the following definition:

$$C^2 = \frac{\chi^2}{N} = \frac{1}{N} \sum_{i=1}^N \left(\frac{F_i - F(\lambda_i; T_{\text{eff}}, \log g, [\text{M}/\text{H}])}{\sigma_i} \right)^2, \quad (1)$$

where $N = 439$ is the number of wavelength points, and F_i and $F(\lambda_i; T_{\text{eff}}, \log g, [\text{M}/\text{H}])$ are the observed and synthetic fluxes, respectively. We assumed $\sigma_i = \sigma_{\text{obs}}$ from Table 1.⁵

The distribution of the computed C^2 values is shown in Figure 3. The generally high C^2 values are probably due to both an underestimate of σ_i and to the nonnormality of the residuals. On the other hand, very high C^2 cast doubt on the *fiducial* parameters themselves. In the following, we will limit our discussion to the 73 stars falling in the dashed area of Figure 3, which comprises 80% of the data ($C^2 < 10$). We point out that the value of 80% for fixing the C^2 threshold is somewhat subjective.

4. THE METALLICITY SCALE

The [Fe/H] distribution for the 73 selected stars is shown in Figure 4. The mean metallicity and standard deviation of

⁵ In the case of only one observed spectrum per star, $\sigma_{\text{obs}} = 0.03$ was assumed.

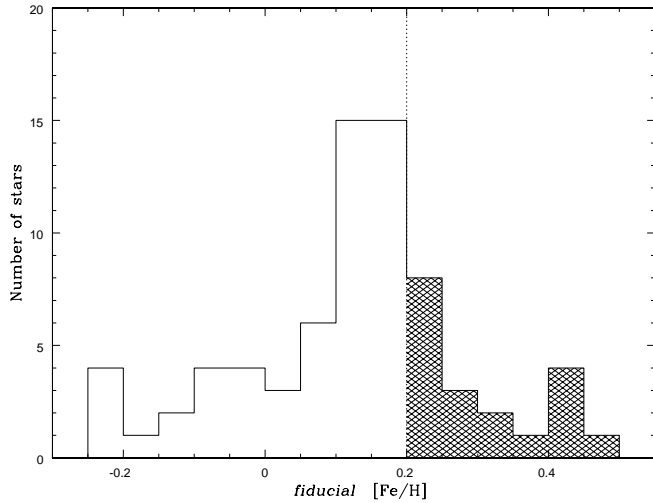


FIG. 4.—Histogram of *fiducial* [Fe/H] values of the 73 stars with $C^2 \leq 10$; the shaded area corresponds to stars with [Fe/H] $\geq +0.2$ dex.

the sample are

$$\langle [\text{Fe}/\text{H}] \rangle = 0.12 \text{ dex}, \quad \sigma = 0.16 \text{ dex}, \quad (2)$$

with 49 stars (67%) with [Fe/H] $\geq +0.1$. The presence of a significant fraction of nonsupermetallicity stars is not completely unexpected, although our sample was selected on the basis of hints of supermetallicity in the literature. Actually, there is a wide spread in the literature parameters, and 39% of the 175 individual [Fe/H] estimates for the 45 stars with more than one CAY97 data set were less than 0.1 dex. This result means that several SMR candidates are actually solar metallicity stars or even metal-poor ones. On the other hand, the presence of stars fulfilling the Taylor (1996) SMR criterion (i.e., [Fe/H] ≥ 0.2) is confirmed. Our sample, in fact, comprises 19 SMR stars with [Fe/H] ranging from 0.20 to 0.49 dex. For these stars, even though the spectral resolution of the observations is not the best suited for detailed analyses, we looked for possible systematic differences between observed and model spectra. The comparison was done in the following wavelength intervals: (1) 5154.125–5196.625 Å, (2) 5245.65–5282.65 Å, (3) 5312.125–5352.125 Å, and (4) 5285.65–5318.15 Å, which correspond to the central bandpasses of Lick narrowband spectrophotometric indices Mg₂, Fe5270, Fe5335, and a quasi-continuum bandpass, respectively. In general, the residuals do not show any significant systematic trend, thus confirming the model predictions of scaled solar abundance.

4.1. μ Leonis

As is well known, the star μ Leo (HD 85503) has received special attention as a reference template of super-metal-rich stars (see, for instance, McWilliam 1997 and Taylor 1999c,

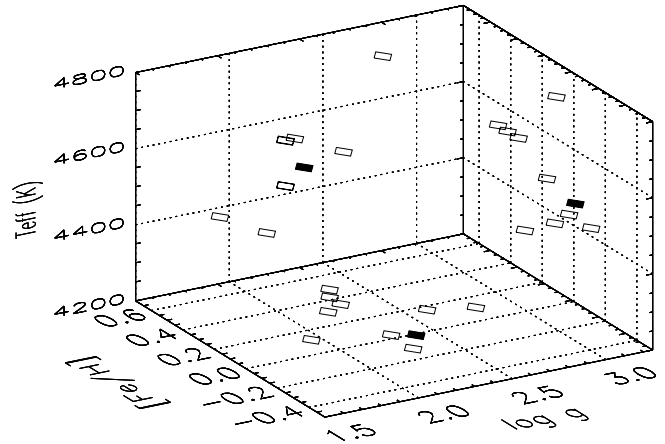


FIG. 5.—Comparison of the atmospheric parameters for μ Leo from CAY97 (open symbols) with the *fiducial* solution from Table 1 (filled symbols).

and references therein). Figure 5 shows the comparison of our *fiducial* parameters with the other nine (T_{eff} , $\log g$, [Fe/H]) determinations reported in Table 1. The spread in the determinations is illustrated by the projections of the parameter sets on the walls of the three-dimensional plot. They span the following ranges: $4308 \leq T_{\text{eff}} \leq 4710$; $1.95 \leq \log g \leq 2.82$; $-0.11 \leq [\text{Fe}/\text{H}] \leq +0.48$. Our *fiducial* set (4460, 2.4, −0.01) falls within the above-mentioned boundaries. Both T_{eff} and $\log g$ are very close to their mean values computed using the other nine sets, while the [Fe/H] is the second lowest value and is not consistent with the SMR hypothesis. Our results are probably affected by our assumption, in obtaining the *fiducial* parameters, of solar partition. This may not be the case for μ Leo. In fact, Castro et al. (1996) derived individual elemental abundances and found hints of deviations from scaled solar partitions ([Fe/H] = +0.46 and “roughly solar Ca and Ti abundances”). Unfortunately, deviations from solar partitions cannot be taken into account by using CMM synthetic spectra; thus our results for this star must be taken with caution.

4.2. The Most Extreme SMR Stars

The spectra of the three most metal-rich stars in our sample, namely, those with [Fe/H] $> +0.4$, are displayed in Figure 6. They are HD 1461 ([Fe/H] = +0.43), HD 52973 ([Fe/H] = +0.49), and HD 61064 ([Fe/H] = +0.44). In the figure, spectra are sorted in the sense of increasing metallicity. These stars are worthy of further discussion, given their relevance to extending the pattern of Galactic metal abundances beyond Z_{\odot} .

HD 1461 = HR 72.—No recent detailed spectroscopy can be found in the literature for this $V = 6.46$ star. The two references in CAY97 (Spinrad & Luebke 1970 and Bell & Branch 1971) are quite old and present metallicity determi-

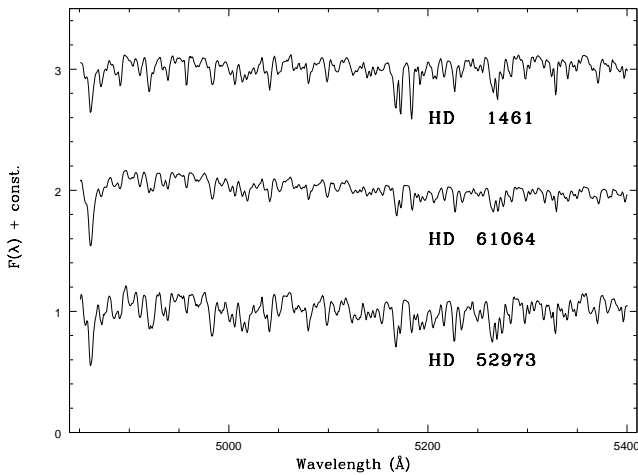


FIG. 6.—Spectra of the three stars in our sample with $[\text{Fe}/\text{H}] > +0.4$. Spectra are sorted in the sense of increasing metallicity (from top to bottom).

nations from curve-of-growth analyses. A much lower value, $[\text{Fe}/\text{H}] = +0.14$, is derived from Strömgren photometry by Eggen (1998).

A comparison of our spectrum with those of HD 114710 and HD 10307, two quasi-solar chemical composition stars in our database with similar T_{eff} and $\log g$ values, can be useful to get a model-independent clue on the differential metal enhancement in HD 1461.

As displayed in Figure 7, the relative flux (in the sense HD 1461—HD 114710 and HD 1461—HD 10307) clearly indicates strong Mg features and Fe lines, thus confirming $[\text{Fe}/\text{H}] \gg 0$ for HD 1461.

$\text{HD } 61064 = \text{HR } 2927 = 25 \text{ Mon}$.—This evolved star has been studied by Berthet (1990). Original echelle spectroscopy covered the blue region (4420 – 5040 Å) comprising lines for 12 atomic species. The Kurucz (1979) model atmo-

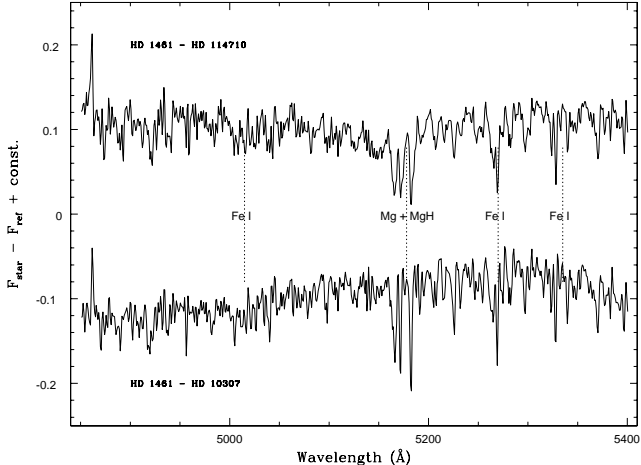


FIG. 7.—Relative spectra of HD 1461 ($[\text{Fe}/\text{H}] = +0.43$) with respect to HD 114710 ($[\text{Fe}/\text{H}] = +0.02$) and to HD 10307 ($[\text{Fe}/\text{H}] = -0.02$), two quasi-solar chemical composition templates with similar temperature and gravity.

spheres provided the theoretical reference framework for the analysis. Indications of deviations from solar partition are present in particular for Y, Zr, Ba, and, possibly, C.

We stress again that CMM spectra are computed by assuming a rigid scaling of element abundances in a solar ratio; therefore, as in the case of μ Leo, our results may be affected by anomalies in individual element abundances.

Venture, Zucker, & Wallerstein (1999) derived a completely different iron abundance, $[\text{Fe}/\text{H}] = -0.3$, assuming $T_{\text{eff}} = 6500$ and $\log g = 3.5$. The corresponding computed CMM synthetic spectrum, compared with our observations, gave an rms error about twice as large as the rmse_{\min} value reported in Table 1, thus suggesting a better agreement of the observations with the SMR hypothesis.

$\text{HD } 52973 = \text{HR } 2650 = \zeta \text{ Gem}$.—The case of HD 52973 is less confident and should be taken with great caution. In fact, because of the low gravity of the star, the assumption of LTE and plane-parallel layers used in computing CMM spectra may not be valid. Moreover, the star is a Cepheid variable, and Fry & Carney (1997) showed that the spectrum at different phases can be reproduced with different values of T_{eff} , $\log g$, and $[\text{M}/\text{H}]$. While variations in T_{eff} and $\log g$ versus phases are expected, the nonuniqueness of the $[\text{M}/\text{H}]$ determination clearly indicates problems in modeling the atmosphere of this star.

5. CONCLUSIONS

In this paper we analyzed a sample of 91 Population I bright stars in the solar neighborhood with at least one reported determination of $[\text{Fe}/\text{H}] \geq +0.1$ from high-resolution spectroscopy in order to study the metallicity scale at supersolar regimes. We identified the photospheric *fiducial* parameters (T_{eff} , $\log g$, $[\text{M}/\text{H}]$) from among published parameter sets via a comparison of new observations in the wavelength range 5034 – 5398 Å with synthetic spectra based on K93 model atmospheres. In particular, we adopted a statistical test in order to provide a measure of the soundness of *fiducial* estimates of the metallicity $[\text{Fe}/\text{H}]$, and found acceptable results for 73 stars of our sample. As a main result of our analysis, we found that the existence of a “genuine” SMR stellar component in the Galactic disk is confirmed, with 19 stars in our sample fulfilling Taylor’s (1996) criterion ($[\text{Fe}/\text{H}] \geq 0.2$ dex) and three stars as metal-rich as $[\text{Fe}/\text{H}] > +0.4$ dex.

This work was partially supported by the Italian MURST (60% and 40% grants, Università degli Studi di Trieste, Osservatorio Astronomico di Trieste and Osservatorio Astronomico di Brera-Milano), and by the Consiglio Nazionale delle Ricerche (CNR-GNA). Partial support from Mexican CONACyT is also acknowledged via grant E9506-0099P-E.

REFERENCES

- Abia, C., & Rebolo, R. 1989, *ApJ*, 347, 186
- Anders, E., & Grevesse, N. 1989, *Geochim. Cosmochim. Acta*, 53, 197
- Barbuy, B. 1988, *A&A*, 191, 121
- Bell, R. A., & Branch, D. 1971, *MmRAS*, 153, 57
- Bell, R. A., & Gustafsson, B. 1978, *A&AS*, 34, 229
- Berthet, S. 1990, *A&A*, 227, 156
- Bessell, M. S., Brett, J. M., Wood, P. R., & Scholz, M. 1989, *A&AS*, 77, 1
- Bessell, M. S., Sutherland, R. S., & Ruan, K. 1991, *ApJ*, 383, L71
- Burstein, D., Faber, S. M., Gaskell, C. M., & Krumm, N. 1984, *ApJ*, 287, 586
- Buser, R., & Kurucz, R. L. 1992, *A&A*, 264, 557
- Castelli, F., Gratton, R. G., & Kurucz, R. L. 1997, *A&A*, 318, 841
- Castro, S., Rich, R. M., McWilliam, A., Ho, L. C., Spinrad, H., Filippenko, A. V., & Bell, R. A. 1996, *AJ*, 111, 2439
- Cayrel de Strobel, G., Soubiran, C., Friel, E. D., Ralite, N., & François, P. 1997, *A&AS*, 124, 299 (CAY97)
- Chavez, M. 1995, Ph.D. thesis, SISSA
- Chavez, M., Buzzoni, A., Malagnini, M. L., & Morossi, C. 1996a, in ASP Conf. Ser. 86, *Fresh Views of Elliptical Galaxies*, ed. A. Buzzoni, A. Renzini, & A. Serrano (San Francisco: ASP), 249
- Chavez, M., Malagnini, M. L., & Morossi, C. 1995, *ApJ*, 440, 210
- . 1996b, *ApJ*, 471, 726
- . 1997, *A&AS*, 126, 267 (CMM)
- Chavez, M., Malagnini, M. L., Morossi, C., & Buzzoni, A. 1996c, in ASP Conf. Ser. 98, *From Stars to Galaxies*, ed. C. Leitherer, U. Fritze, & J. Huchra (San Francisco: ASP), 100
- Edvardsson, B., Andersen, J., Gustafsson, B., Lambert, D. L., Nissen, P. E., & Tomkin, J. 1993, *A&A*, 275, 101
- Eggen O. J. 1998, *AJ*, 115, 2397
- Frogel, J. A. 1999, in *When and How Do Bulges Form and Evolve?* ed. M. Carollo, H. C. Ferguson, & R. F. G. Wyse (Cambridge: Cambridge Univ. Press), in press (astro-ph/9903071)
- Fry, A. M., & Carney, B. W. 1997, *AJ*, 113, 1073
- Geisler, D., & Friel, E. D. 1992, *AJ*, 104, 128
- Gratton, R. G., & Ortolani, S. 1986, *A&A*, 169, 201
- Gulati, R. K. 1989, M.Phil. thesis, SISSA
- . 1991, Ph.D. thesis, SISSA
- Gulati, R. K., Malagnini, M. L., & Morossi, C. 1993, *ApJ*, 413, 166
- Gutiérrez-Moreno, A., Moreno, H., Cortés, G., & Wenderoth, E. 1988, *PASP*, 100, 973
- Image Reduction and Analysis Facility. 1992, Version 2.10.1 (Tucson: NOAO)
- Kurucz, R. L. 1979, *ApJS*, 40, 1
- . 1993, CD-ROM 13, *ATLAS9 Stellar Atmosphere Programs and 2 km/s Grid* (Cambridge: SAO) (K93)
- Kurucz, R. L., Furenlid, I., Brault, J., & Testerman, L. 1984, *Solar Flux Atlas from 296 to 1300 nm* (Sunspot: NSO), 240
- Malagnini, M. L., Morossi, C., Buzzoni, A., & Mantegazza, L. 1994, *Mem. Soc. Astron. Italiana*, 65, 803
- McWilliam, A. 1997, *ARA&A*, 35, 503
- McWilliam, A., & Rich, R. M. 1994, *ApJS*, 91, 749
- Montes, D., Ramsey, L. W., & Welty, A. D. 1999, *ApJS*, 123, 283
- Rich, R. M. 1988, *AJ*, 95, 828
- Sadler, E. M., Rich, R. M., & Terndrup, D. M. 1996, *AJ*, 112, 171
- Spinrad, H., & Luebke, W. R. 1970, *ApJ*, 160, 1141
- Spinrad, H., & Taylor, B. J. 1969, *ApJ*, 157, 1279
- Taylor, B. J. 1991, *ApJS*, 76, 715
- . 1994a, *PASP*, 106, 704
- . 1994b, *PASP*, 106, 590
- . 1995, *PASP*, 107, 734
- . 1996, *ApJS*, 102, 105
- . 1999a, *A&AS*, 134, 523
- . 1999b, *A&AS*, 135, 75
- . 1999c, *A&A*, 344, 655
- Terndrup, D. M., Frogel, J. A., & Whitford, A. E. 1991, *ApJ*, 378, 742
- Trippico, M. J., & Bell, R. A. 1990, *AJ*, 99, 691
- . 1995, *AJ*, 110, 3035
- Tsuji, T. 1978, *A&A*, 62, 29
- Venture, A. D., Zucker, D., & Wallerstein, G. 1999, *PASP*, 111, 84
- Whitford, A. E., & Rich, R. M. 1983, *ApJ*, 274, 723
- Worthey, G., Faber, S. M., Gonzalez, J. J., & Burstein, D. 1994, *ApJS*, 94, 687